Effect of Vinyl Acetate Content on the Mechanical and Thermal Properties of Ethylene Vinyl Acetate/MgAl Layered Double Hydroxide Nanocomposites

T. Kuila,[1] H. Acharya,[1] S. K. Srivastava,[1] A. K. Bhowmick[2]

[1]*Inorganic Materials and Nanocomposite Laboratory, Department of chemistry, Indian Institute of Technology, Kharagpur 721302, India*
[2]*Rubber Technology Centre, Indian Institute Technology, Kharagpur 721302, India*

Received 23 May 2007; accepted 28 November 2007
DOI 10.1002/app.27834
Published online 23 January 2008 in Wiley InterScience (www.interscience.wiley.com).

ABSTRACT: Ethylene vinyl acetate (EVA)/Mg-Al layered double hydroxide (LDH) nanocomposites using EVA of different vinyl acetate contents (EVA-18 and EVA-45) have been prepared by solution blending method. X-ray diffraction and transmission electron microscopic studies of nanocomposites clearly indicate the formation of exfoliated/intercalated structure for EVA-18 and completely delaminated structure for EVA-45. Though EVA-18 nanocomposites do not show significant improvement in mechanical properties, EVA-45 nanocomposites with 5 wt % DS-LDH content results in tensile strength and elongation at break to be 25% and 7.5% higher compared to neat EVA-45. The data from thermogravimetric analysis show that the nanocomposites of EVA-18 and EVA-45 have $\approx 10^{\circ}C$ higher thermal decomposition temperature compared to neat EVA. © 2008 Wiley Periodicals, Inc. J Appl Polym Sci 108: 1329–1335, 2008

Key words: EVA; nanocomposites; morphology; TEM; mechanical properties; TGA

INTRODUCTION

In recent years, polymer/layered inorganic nanocomposites have attracted great research interest in the field of materials chemistry because of their novel mechanical, thermal, gas barrier, and optical properties.[1–4] The improvement of these properties compared to neat polymer, depends on the dispersion of inorganic nanofiller in the polymer matrix and the compatibility between the inorganic filler and organic polymer.[5] So far, investigations have been mainly focused on the cationic clays, especially montmorillonites (MMT).[6–11] However, layered double hydroxides (LDH) for such systems have been studied less.[12,13] LDHs are anionic clays with positively charged metal oxide/hydroxide layers with anions for charge neutralization. The positive charge is originated by the substitution of the divalent cation by trivalent one. The general chemical formula of LDHs is $[M^{II}_{(1-x)}M^{III}_{x}(OH)_2]^{x+}A^{m-}_{x/m} \cdot nH_2O$, where M^{2+} is divalent cation such as Mg^{2+}, Zn^{2+}, etc., M^{3+} is trivalent cation such as Al^{3+}, Cr^{3+}, etc., and A is an anion with valency m (like Cl^-, CO_3^{2-}, SO_4^{2-}, and NO_3^- etc.). Because of its strong electrostatic attraction between the LDH layers and short interlayer distance ($\sim$ 0.76 nm), it is difficult to exfoliate the LDHs by the polymer chain. But fortunately previous work shows that after appropriate surface modification, LDH may be exfoliated and homogeneously dispersed in polymer matrix to get polymer/LDH nanocomposites.[5,13]

Generally, two kinds of polymer/LDH nanocomposite are obtained depending on the distribution of filler in the polymer matrix.[13] In intercalated nanocomposites, the polymer chains are inserted in between the LDH layers, resulting in well-ordered multilayer morphology with alternating polymeric and LDH layers. When the individual LDH layers are completely delaminated into nanometer-sized single layers, i.e., dispersed homogeneously in the polymer matrix, an exfoliated or delaminated polymer/LDH nanocomposite is obtained. In between these two types of nanocomposites, the later one usually attracts more interest because of nanoscale dispersion of LDH layers in polymer matrix and thereby showing enhanced properties compared to intercalated nanocomposite.[13] Earlier studies show that LDH/polymer nanocomposites can be synthesized by two methods: solution intercalation[14,15] and melt intercalation process.[13,16] But solution intercalation process have invariably been used, for example, *in situ* polymerization,[17,18] direct intercalation in polymer solution[19,20] due to the better dispersion of nanofiller in the polymer matrix.[21]

Correspondence to: S. K. Srivastava (sunit@chem.iitkgp.ernet.in).

Contract grant sponsors: CSIR, DRDO (New Delhi).

Ethylene vinyl acetate (EVA) is one of the important organic polymers, extensively used for the application of electrical insulation purpose, cable jacketing and repair, component encapsulation and water proofing, corrosion protection, and packaging of component. However, bulk EVA does not often fulfill the requirements in terms of its thermal stability behavior and mechanical properties in some specific areas. Thus, to improve these properties some nanomaterial can be added as filler. The successful application of organomodified clay specially MMT,[6–11,22,23] nano $Mg(OH)_2$ [24] in making EVA nanocomposites are well established. LDH is another alternative promising material, which can be used for the synthesis of EVA/LDH nanocomposite to find out the improvements in mechanical properties, thermal stability behavior, and their possible uses for fire retardancy. The present work, therefore, is focused on the exfoliation of Mg-Al LDH nanolayers with EVA matrix and the effect of filler loading on the mechanical and thermal properties of EVA/DS-LDH nanocomposites. The effect of vinyl acetate content is also highlighted here.

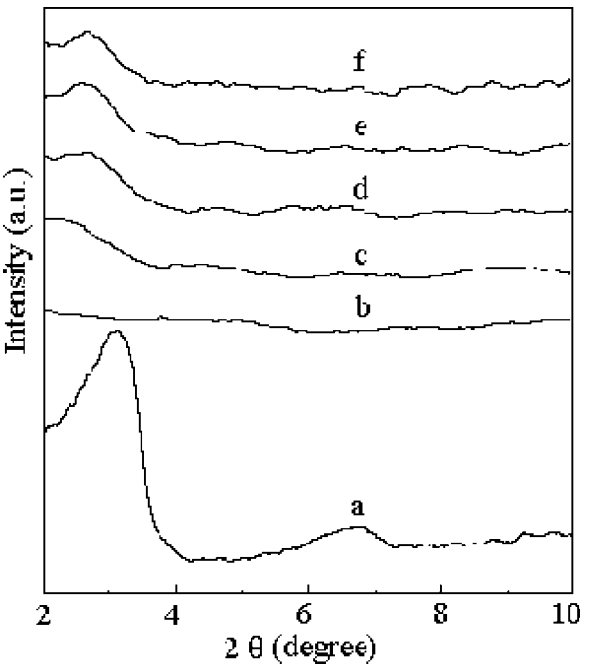

Figure 1 XRD spectra of (a) DS-LDH, (b) EVA-18, (c) EVA-18/DS-LDH (1 wt %), (d) EVA-18/DS-LDH (3 wt %), (e) EVA-18/DS-LDH (5 wt %), (f) EVA-18/DS-LDH (8 wt %).

EXPERIMENTAL

Materials

EVA with vinyl acetate content of 18 wt % was obtained from Reliance Industries, Mumbai, India (EVA 1802; melt flow index = 2 g/10 min; density at 23°C = 936 kg/m^3). EVA with 45 wt % vinyl acetate was supplied by Bayer Corp., Germany (Levamelt 450; melt flow index = 3 ± 2 g/10 min). The crosslinking agent dicumyl peroxide (DiCUP-98, from Hercules, U.S.) was used to prepare the sheets of neat EVA samples and their nanocomposites. $Mg(NO_3)_2 \cdot 6H_2O$, $Al(NO_3)_3 \cdot 9H_2O$, and Na_2CO_3 were purchased from E. Merck, India. Sodium hydroxide (Quest Chemicals, Kolkata, India) and sodium dodecyl sulfate (SRL, Mumbai, India) were used to prepare DS intercalated LDH. Toluene was used as solvent and purchased from SRL, Mumbai, India.

Preparation of Mg-Al LDH

Mg/Al LDH precursor was prepared following co-precipitation method.[21] In 100 mL water, $Mg(NO_3)_2 \cdot 6H_2O$ (0.25 mol, 19.65 g) and $Al(NO_3)_3 \cdot 9H_2O$ (0.75 mol, 9.25 g) were added and dissolved completely. The mixed metal nitrate solution obtained was slowly added to an aqueous solution containing 0.25 mol (2.65 g) Na_2CO_3 and 0.2 mol (8 g) NaOH under stirring condition. During addition, the solution pH is maintained at 8 to 9 with 1 mol/L aqueous NaOH solution. The resulting white precipitate was then aged for 16 h at 75°C ± 5°C, and finally filtered, washed with distilled water and dried in air at room temperature for 24 h and then followed by 24 h under vacuum at 80°C. The organophilic LDH was obtained by rehydration of calcined MgAl LDH. For this, 2.5 g LDH was calcined at 500°C for 6 h, and then suspended in a 100 mL aqueous solution containing 2.5 g of SDS. The suspended solution was stirred for 12 h at 70°C and then refluxed for another 6 h to yield a white powder of organophilic LDH (DS-LDH).

Preparation of EVA/LDH nanocomposites

The nanocomposites of EVA-18 and EVA-45 with different amount of DS-LDH (1, 3, 5, and 8 wt %) were prepared by solution intercalation process. This method involved refluxing of desired amount of DS-LDH in 30 mL toluene at 100°C for 6 h. Subsequently, the dispersion so obtained was added to the solution of 15 g of EVA already dissolved in 100 mL toluene and stirred vigorously for 6 h at 100°C. Finally, DCP as curing agent was added to this and subsequently the solvent was extracted under reduced pressure and the resultant composites were roll milled at room temperature followed by compression molding at 150°C for 45 min.

Characterization

X-ray diffraction (XRD) studies of the samples were carried out using a PANalytical (PW 3040/60),

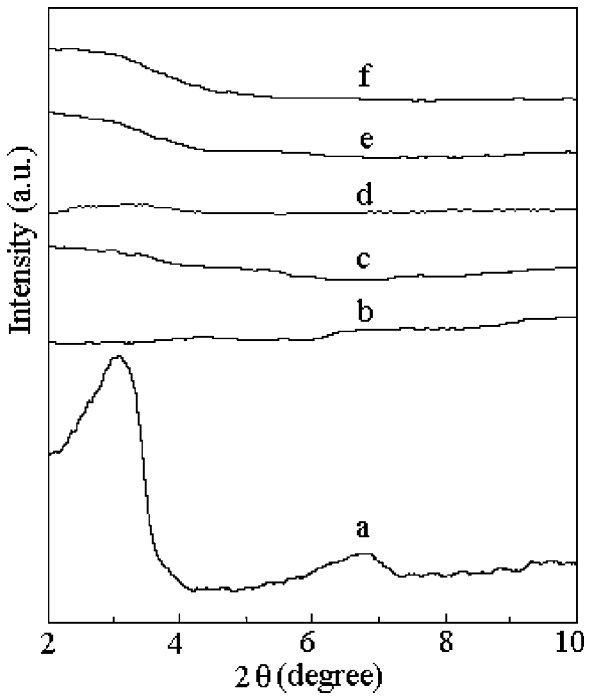

Figure 2 XRD spectra of (a) DS-LDH, (b) EVA-45, (c) EVA-45/DS-LDH (1 wt %), (d) EVA-45/DS-LDH (3 wt %), (e) EVA-45/DS-LDH (5 wt %), (f) EVA-45/DS-LDH (8 wt %).

model 'X' Pert Pro with Cu K_α radiation (λ = 1.541 Å). The scanning range was 2–10° with a scanning rate of 3°/min. Dispersion of DS-LDH in EVA matrix was analyzed using a JEOL 2100 200 KV transmission electron microscope (TEM). For the tensile measurement, the test specimen conforming to ASTM D412 was cut out from the compression molded sheets of virgin polymers and the nanocomposites. The tensile properties were recorded on a Zwick/Roell Z010 at a strain rate of 100 mm/min at 25°C ± 2°C. The tensile fractured surface of the samples was gold coated under argon atmosphere, and the fractured morphology was recorded using scanning electron microscope (SEM), JEOL (JSM-5800) with an acceleration voltage of 20 kV. Thermogravimetric analysis of the neat polymer and the nanocomposites were carried out on Redcroft 870 thermal analyzer, Perkin-Elmer with a heating rate of 10°C/min over a temperature range of 60–600°C in air atmosphere. The initial weight taken for this analysis was ~ 5 mg for each sample.

RESULTS AND DISCUSSION

XRD analysis

Figure 1 shows the XRD patterns of DS-LDH, EVA-18, and the EVA-18 nanocomposites with different amounts of DS-LDH content. The interlayer spacing of d_{001} plane of DS-LDH is found to be 2.76 nm. It is also clear from Figure 1 that the original peak (d_{001}) of DS-LDH is shifted to lower angle corresponding to an interlayer distance of 4.08 nm in the nanocomposites. The increase in *d*-spacing for EVA-18 nanocomposites is due to the intercalation of polymer chains into the gallery spaces of DS-LDH.[18]

XRD patterns for the polymeric nanocomposites with 45 wt % vinyl acetate (VA) content and DS-LDH are displayed in Figure 2. The original peak

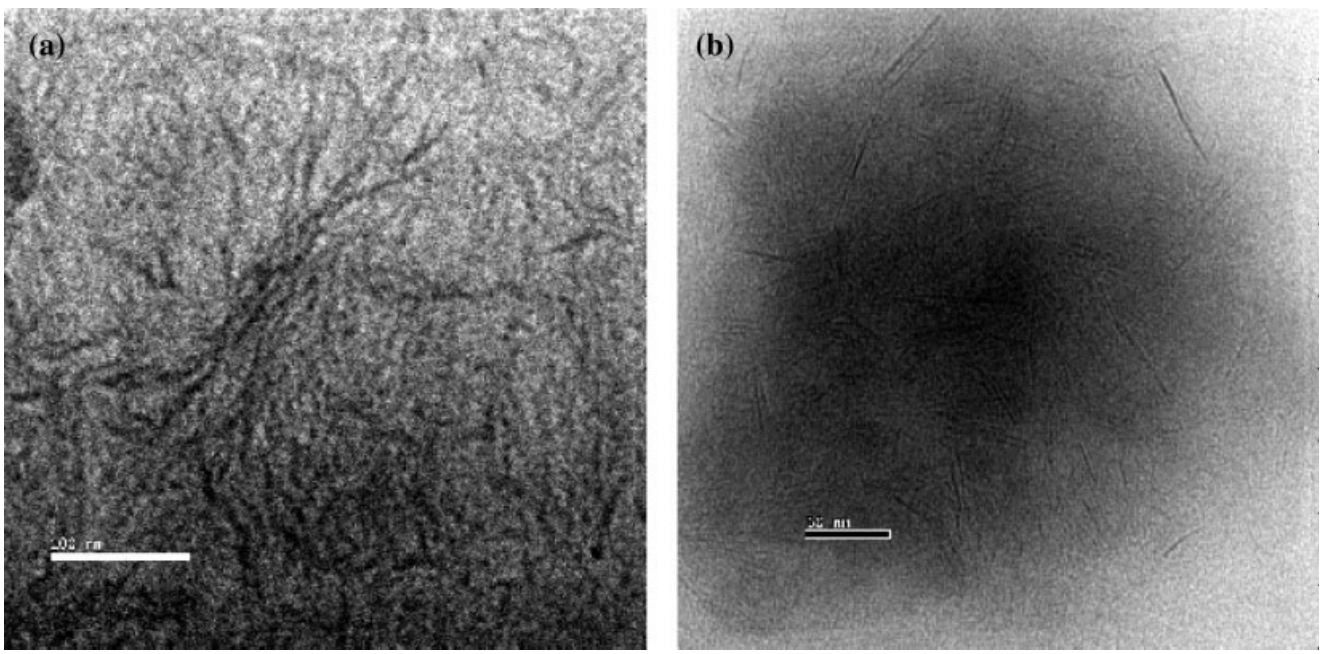

Figure 3 TEM images of (a) EVA-18/DS-LDH (1 wt %) and (b) EVA-45/DS-LDH (5 wt %) nanocomposites.

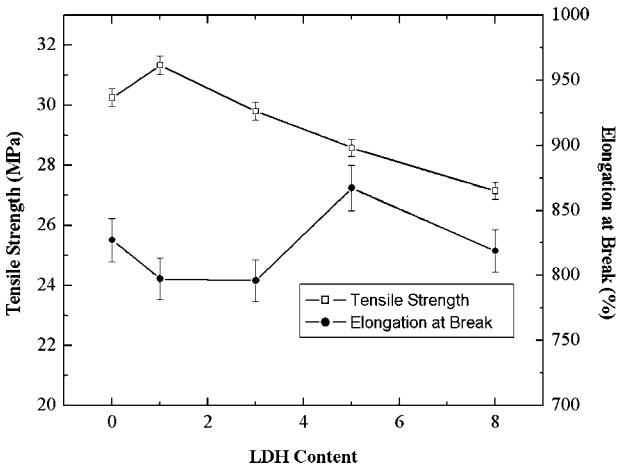

Figure 4 Variation of TS and EB (%) of EVA-18/DS-LDH nanocomposites.

(d_{001}) of DS-LDH is absent for all EVA-45/DS-LDH nanocomposites. This indicates that the LDH platelets are either randomly oriented or separated far enough to produce insignificant diffraction peaks.[25] This is possibly due to the insertion of a larger number of polymeric chain into the intergallery space of LDH. This is also anticipated that the polar interaction between VA and DS-LDH plays an important role on the intercalation of polymer inside the LDH layers. Moreover, with increasing the VA content in EVA copolymer, thermodynamic energy barrier for intercalation decreases. As a result, more number of polymeric chains will intercalate within the LDH platelets suggesting that the system has achieved exfoliated state.

TEM analysis

TEM is one of the most important tools to study the dispersion of LDH nanolayers in the polymer matrix.

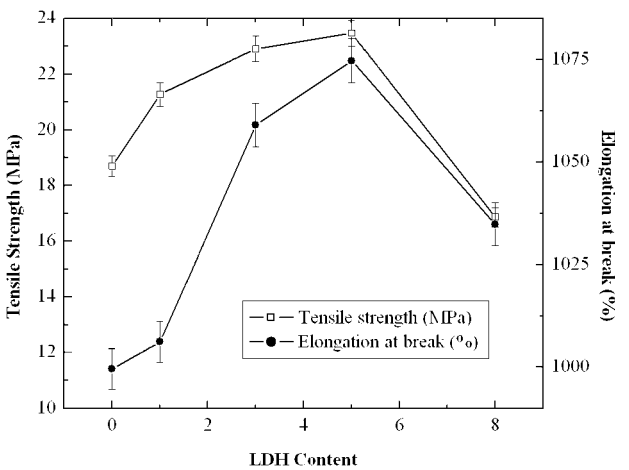

Figure 5 Variation of TS and EB (%) of EVA-45/DS-LDH nanocomposites.

Figure 3(a) displays the TEM micrographs for EVA-18 nanocomposites with 1 wt % DS-LDH. The TEM image reveals very complex nature of morphology where the dispersed LDH particles vary widely in shapes and sizes and the LDH layers are completely delaminated and their distribution is homogeneous.

TEM images of EVA-45/DS-LDH nanocomposite with 5 wt % DS-LDH is shown in Figure 3(b). It is evident from the TEM images that the stacked LDH layers lose their ordered layer-structures and are distributed randomly in the EVA-45 matrix. The thickness and lateral size of exfoliated LDH layers are about 1 nm and 40–60 nm, respectively. These observations are also consistent with those from XRD analysis.

Mechanical properties

The variation of tensile strength (TS) and elongation at break (EB) for the nanocomposites of EVA-18 and EVA-45 with different amount of DS-LDH are presented in Figures 4 and 5. It can be noted that the TS for EVA-18 nanocomposite with 1 wt % DS-LDH content is improved compared to neat EVA-18. But, further addition of DS-LDH causes reduction of TS. It therefore appears that at low filler loading, the reinforcement of EVA-18 by DS-LDH is maximum. However, at higher filler loading, some agglomeration is likely to occur which suppresses the reinforcing effect of DS-LDH and which ultimately leads to decrease of TS. It is also evident from Figure 4 that the EB first decreases with the addition of DS-LDH in EVA-18, and then increases to some extent when the content of nanofiller in EVA-18 is 5 wt %. Such an improvement in EB may be due to the platelet orientation of LDH nanolayers.[21] While for EVA-45

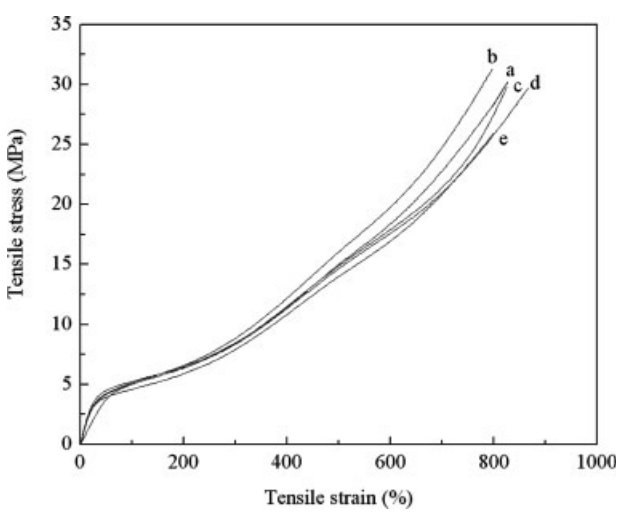

Figure 6 Stress versus strain plot of (a) EVA-18, (b) EVA-18/DS-LDH (1 wt %), (c) EVA-18/DS- LDH (3 wt %), (d) EVA-18/DS-LDH (5 wt %), (e) EVA-18/DS-LDH (8 wt %).

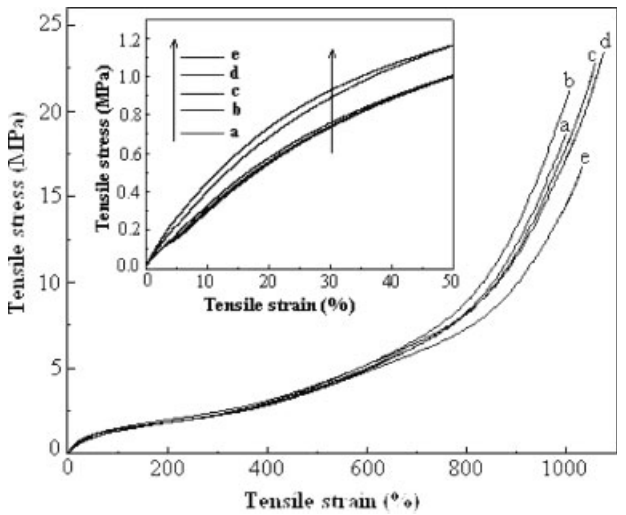

Figure 7 Stress versus strain plot of (a) EVA-45, (b) EVA-45/DS-LDH (1 wt %), (c) EVA-45/DS- LDH (3 wt %), (d) EVA-45/DS-LDH (5 wt %), (e) EVA-45/DS-LDH (8 wt %).

(Fig. 5), the TS and EB for the nanocomposite containing 5 wt % DS-LDH compared to neat EVA-45 increases from 18.6 MPa to 23.4 MPa and 999 to 1074, respectively. This increase of TS and EB is possibly due to the good compatibility between the polymer matrix and the inorganic nanolayers. The interfacial interaction between the VA of EVA-45 and hydroxyl group of DS-LDH is much more compared to EVA-18, because of the presence of higher amount of VA. Such well dispersed DS-LDH nanolayers effectively enhance the TS of the EVA-45/DS-LDH nanocomposites, though its value decreases when the DS-LDH content exceed 5 wt %.

Figures 6 and 7 shows stress–strain curves for the raw polymer and the nanocomposites of EVA-18 and EVA-45 with different amount of DS-LDH. The nanocomposite of EVA-18 with 1 wt % DS-LDH shows higher tensile modulus as evident from Figure 6. However, further addition of filler results in the reduction of tensile modulus of EVA-18/DS-LDH nanocomposites. It can be noted from Figure 7

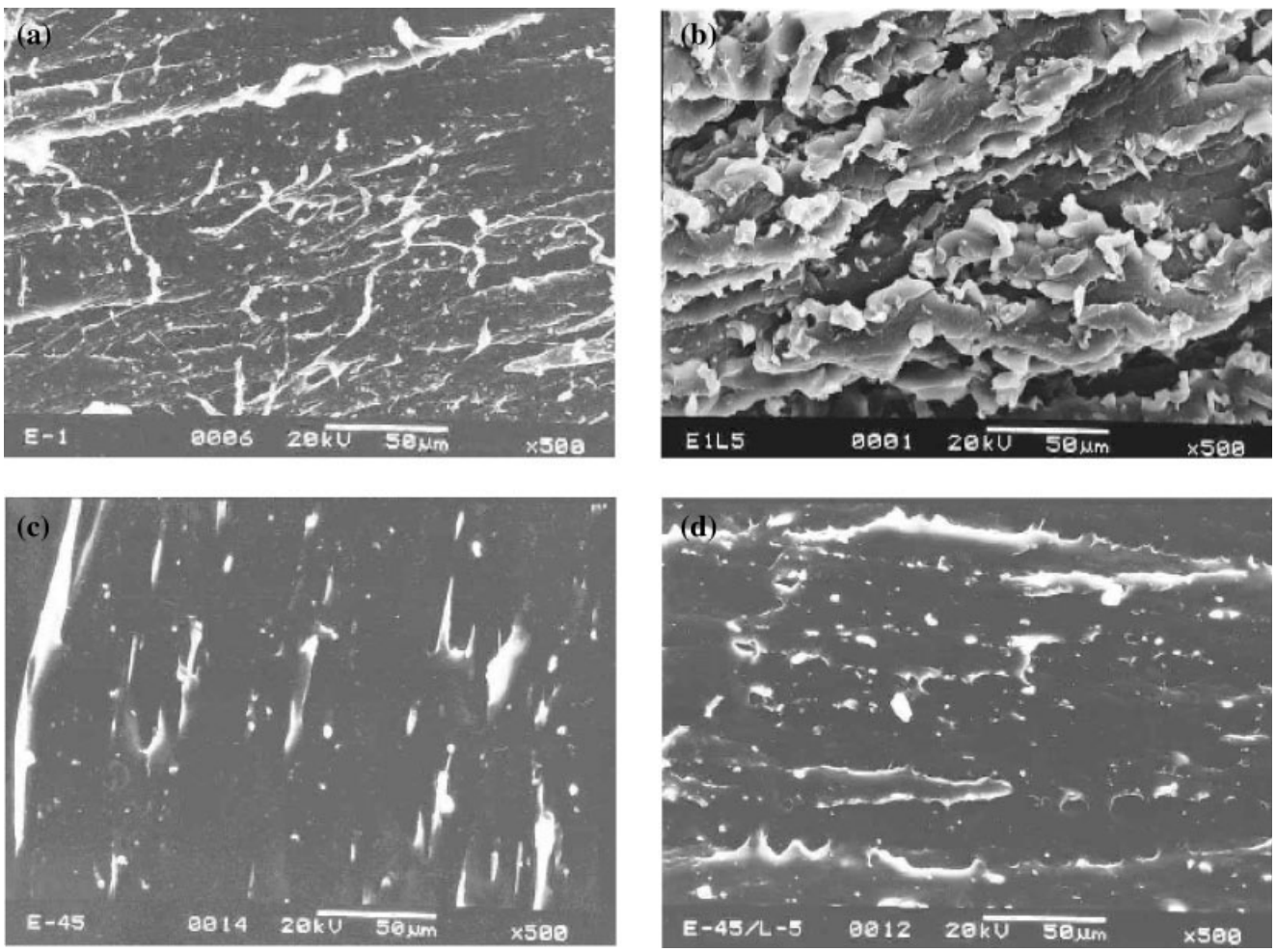

Figure 8 Tensile fracture surface morphology of (a) EVA-18, (b) EVA-18/DS-LDH (5 wt %), (c) EVA-45, (d) EVA-45/DS-LDH (5 wt %).

that the tensile modulus for the nanocomposite with 1 wt % DS-LDH content at any elongation is higher compared to neat EVA-45. However, at lower elongation (50%), the tensile modulus is always higher for the nanocomposites. The enhanced tensile modulus for the nanocomposites is possibly due to the formation of some shear zones when the nanocomposites are under stress and strain conditions.[26]

Fracture surface morphology

The tensile-fractured morphology of EVA-18 and EVA-18/DS-LDH (5 wt %) nanocomposites are shown in Figure 8(a,b). The fractured surfaces of neat EVA-18 shows some cracks, while the nanocomposites containing 5 wt % DS-LDH does not show any prominent cracks. This is possibly due to the formation of some shear zones which reduces the formation of cracks and ultimately toughened the nanocomposites materials.[21]

Figure 8(c,d) shows the SEM micrographs of the tensile-fractured surfaces of EVA-45 and EVA-45/DS-LDH (5 wt %) nanocomposites. The fracture morphology of the composites with 5 wt % DS-LDH is totally different from that of neat EVA-45. Considering the tensile mechanical data, it seems that rougher the fracture surface, better the mechanical properties of the related nanocomposite. Such type of surface morphology variation is possibly due to the deviation of tear. It is also inferred from the SEM images that DS-LDH is compatible with EVA-45, and possibly its platelet orientation is likely to account for improved mechanical properties in the corresponding nanocomposites.

Thermogravimetric analysis

Figures 9 and 10 show thermogravimetric curves for the nanocomposites of EVA-18 and EVA-45 with varying amounts of DS-LDH. It is evident that the thermal degradation of EVA takes place in two stages.[27,28] The first step corresponds to the elimination of acetate groups of EVA side chains, taking place in the range of 225–420°C and 214–422°C for EVA-18 and EVA-45, respectively. The second stage is due to the degradation of main chain and occurs at about 420–520°C for EVA-18 and 415–525°C for EVA-45. It is also seen from the Figures that the decrease in initial decomposition temperature for the nanocomposites is accompanied by simultaneous increase in initial weight loss. This is possibly due to the early degradation of DS anion present in organo-LDH.[29] Such an initial weight loss in the nanocomposites is anticipated to reinforce the charring process and may be more useful for the fire safety of the nanocomposites. According to Chen et al.,[17] an efficient charring process in a flame retardant polymer occurs at a temperature higher than its processing temperature but much lower than its decomposition temperature. It is also evident from Figures 9 and 10 that the final decomposition temperature is ≈10°C higher for the nanocomposites compared to neat EVA, and the weight loss at this stage of degradation significantly decreases with the addition of DS-LDH. This is possibly due to the good dispersion of LDH in these nanocomposites and the degradation perhaps only occurs at surface of the nanocomposites to form the char between the sheets of LDH, which can effectively prevent the emission of thermally degraded small gaseous molecules, which

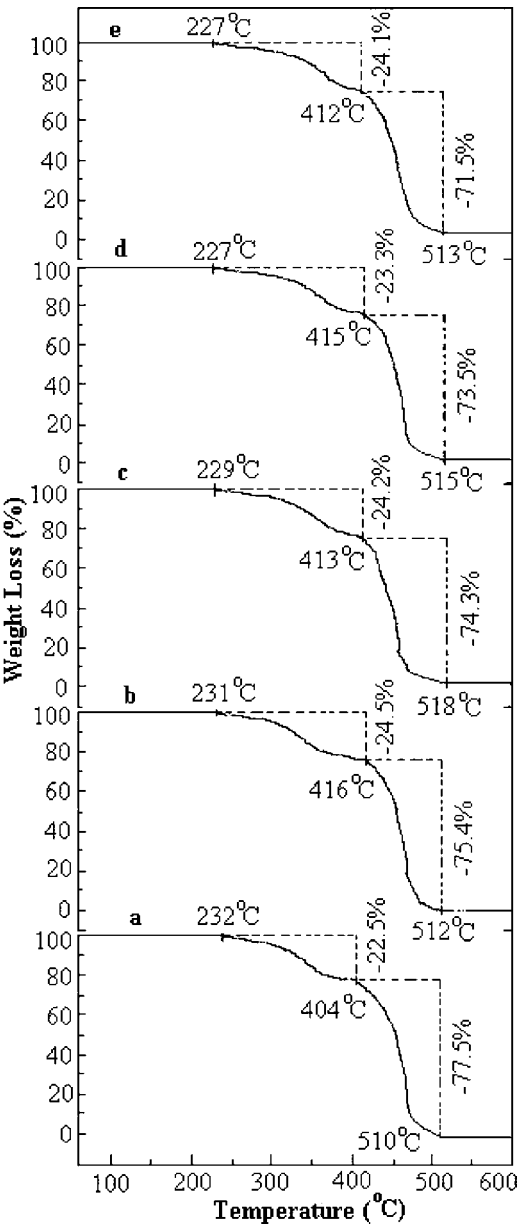

Figure 9 TGA curves of (a) EVA-18, (b) EVA-18/DS-LDH (1 wt %), (c) EVA-18/DS-LDH (3 wt %), (d) EVA-18/DS-LDH (5 wt %), (e) EVA-18/DS-LDH (8 wt %).

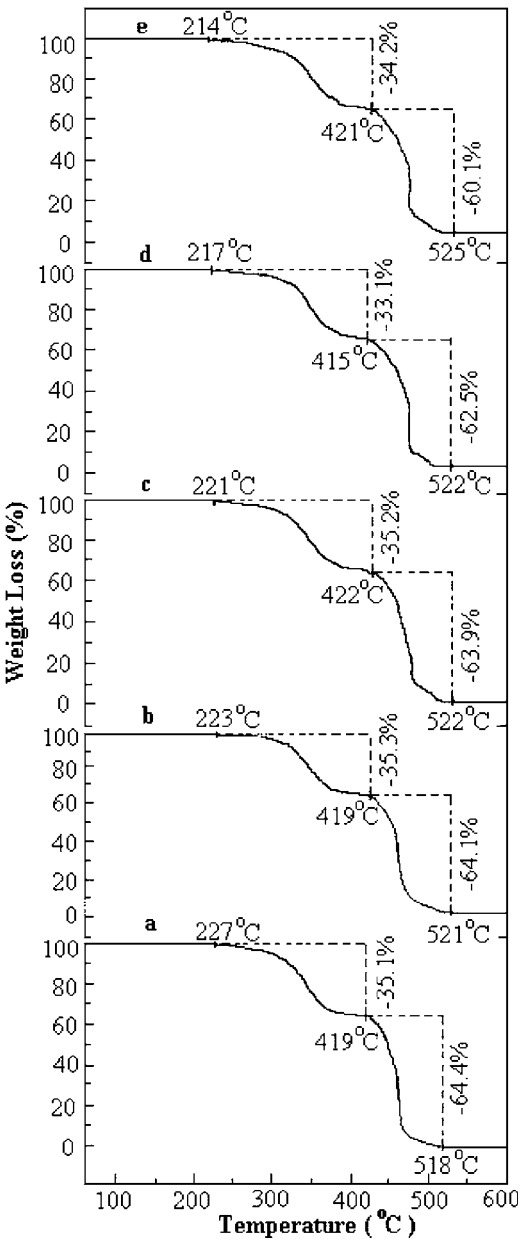

Figure 10 TGA curves of (a) EVA-45, (b) EVA-45/DS-LDH (1 wt %), (c) EVA-45/DS-LDH (3 wt %), (d) EVA-45/DS-LDH (5 wt %), (e) EVA-45/DS-LDH (8 wt %).

ultimately enhance the thermal decomposition temperature of the nanocomposites.

CONCLUSIONS

A significant influence of VA content on the mechanical and thermal properties of EVA/MgAl LDH nanocomposites has been observed. It is clearly evident from XRD and TEM analysis that EVA-18 forms mixed intercalated/exfoliated nanocomposites for higher filler loading, whereas EVA-45 forms completely delaminated nanocomposites. DS-LDH has no significant influence on the mechanical properties of EVA-18. But the nanocomposites of EVA-45 with 5 wt % DS-LDH shows maximum TS and EB compared to neat EVA-45. Thermogravimetric analysis shows that the thermal stability of the nanocomposites of both EVA-18 and EVA-45 is relatively higher and may be used as fire safety materials.

References

1. Alexandre, M.; Dubonis, P. Mater Sci Eng R 2000, 28, 1.
2. Kim, Y.; Choi, Y. S.; Wang, M. H.; Chung, I. J Chem Mater 2002, 14, 4990.
3. Bharadwaj, R. K.; Mehrabi, A. R.; Hamilton, C.; Trujillo, C.; Murga, M.; Fan, R.; Chavira, A.; Thompson, A. K. Polymer 2002, 43, 3699.
4. Chen, G. X.; Choi, J. B.; Yoon, J. S. Macromol Rapid Commun 2005, 26, 183.
5. Lee, W. D.; Im, S. S.; Lim, H.-M.; Kim, K.-J. Polymer 2006, 47, 1364.
6. Sadhu, S.; Bhowmick, A. K. J Mater Sci 2005, 40, 1633.
7. Srivastava, S. K.; Pramanik, M.; Acharya, H. J Polym Sci Part B: Polym Phys 2006, 44, 471.
8. Peeterbroeck, S.; Alexandre, M.; Jerome, R.; Dubois, Ph. Polym Degrad Stab 2005, 90, 288.
9. Maiti, M.; Sadhu, S.; Bhowmick, A. K. J Appl Polym Sci 2006, 101, 603.
10. Sadhu, S.; Bhowmick, A. K. J Polym Sci Part B: Polym Phys 2004, 42, 1573.
11. Maiti, M.; Bhowmick, A. K. Polymer 2006, 47, 6156.
12. Costa, F. C.; Abdel-Goad, M.; Wagenknecht, U.; Heinrich, G. Polymer 2005, 46, 4447.
13. Ding, P.; Qu, B. J Polym Sci Part B: Polym Phys 2006, 44, 3165.
14. Hsueh, H. B.; Chen, C. Y. Polymer 2003, 44, 1151.
15. Qiu, L.; Chen, W.; Qu, B. Polymer 2005, 47, 922.
16. Du, L.; Qu, B.; Zhang, M. Polym Degrad Stab 2007, 92, 497.
17. Leroux, F.; Besse, J. P. Chem Mater 2001, 13, 3507.
18. Chen, W.; Qu, B. Polym Degrad Stab 2005, 90, 162.
19. Chen, W.; Feng, L.; Qu, B. J Chem Mater 2004, 16, 368.
20. Chen, W.; Qu, B. Chem Mater 2003, 15, 3208.
21. Kuila, T.; Acharya, H.; Srivastava, S. K.; Bhowmick, A. K. J Appl Polym Sci 2007, 104, 1845.
22. Suh, S.; Ryu, S. H.; Bae, J. H.; Chang, Y. W. J Appl Polym Sci 2004, 94, 1057.
23. Alexandre, M.; Beyer, G.; Henrist, C.; Cloots, R.; Rulmont, A.; Jerome, R.; Dubois, P. Macromol Rapid Commun 2001, 22, 643.
24. Jiao, C. M.; Wang, Z. Z.; Ye. Z.; Hu, Y.; Fan, W. C. J Fire Sci 2006, 24, 47.
25. Chaudhary, D. S.; Prasad, R.; Gupta, R. K.; Bhattacharya, S. N. Polym Eng Sci 2005, 45, 889.
26. Acharya, H.; Pramanik, M.; Srivastava, S. K.; Bhowmick, A. K. J Appl Polym Sci 2004, 93, 2429.
27. Chattopadhay, S.; Chaki, T. K.; Bhowmick, A. K. J Appl Polym Sci 2001, 81, 1936.
28. Pramanik, M.; Srivastava, S. K.; Samantaray, B. K.; Bhowmick, A. K. J Appl Polym Sci 2003, 87, 2216.
29. Chen, W.; Qu, B. J Mater Chem 2004, 14, 1705.